Modulation of emission and singlet oxygen photosensitisation in live cells utilising bioorthogonal phosphorogenic probes and protein tag technology

Leung, Peter Kam-Keung; Lo, Kenneth Kam-Wing

Published in:
Chemical Communications

Published: 07/06/2020

Document Version:
Post-print, also known as Accepted Author Manuscript, Peer-reviewed or Author Final version

Published version (DOI):
10.1039/d0cc02056g

Publication details:
Leung, P. K.-K., & Lo, K. K.-W. (2020). Modulation of emission and singlet oxygen photosensitisation in live cells utilising bioorthogonal phosphorogenic probes and protein tag technology. *Chemical Communications*, *56*(45), 6074-6077. https://doi.org/10.1039/d0cc02056g

This is the accepted version of a paper published in *Chemical Communications*. This paper has been peer-reviewed but does not include the final publisher proof-corrections or journal pagination.

Leung, P. K-K., & Lo, K. K-W. (2020). Modulation of emission and singlet oxygen photosensitisation in live cells utilising bioorthogonal phosphorogenic probes and protein tag technology. *Chemical Communications, 56*(45), 6074-6077. https://doi.org/10.1039/d0cc02056g.

COMMUNICATION

Modulation of emission and singlet oxygen photosensitisation in live cells utilising bioorthogonal phosphorogenic probes and protein tag technology†

Received 00th January 20xx,
Accepted 00th January 20xx

DOI: 10.1039/x0xx00000x

Peter Kam-Keung Leung[a] and Kenneth Kam-Wing Lo*[abc]

Herein we report a strategy to utilise the bioorthogonal reactivity and phosphorogenic property of iridium(III) polypyridine nitrone complexes and SNAP-tag protein for the modulation of emission and singlet oxygen ($^1O_2$) photosensitisation in live cells.

SNAP-tag is a self-labelling protein that is commonly fused to a protein of interest (POI) as a tag to study cellular localisation and protein functions.[1] It has a cysteine residue that undergoes specific nucleophilic reactions with substrates containing a benzylguanine (BG) moiety, resulting in irreversible covalent labelling.[2] To date, a number of organic dyes have been modified with BG to afford fluorescent probes; for example, SNAP-tag substrates have been used as photoswitchable dyes for super-resolution imaging,[3] probes for dynamic tracking of protein translocation,[4] crosslinking agents to study protein-protein interaction,[5] sensors for localised ion detection,[6] and photosensitisers for chromophore-assisted light inactivation (CALI).[7] Importantly, some of these substrates exhibit fluorescence enhancement upon conjugation to SNAP-tag.[8,9] These fluorogenic probes allow the visualisation of the POI in high resolution without the requirement of stringent washing steps to remove unreacted probes.[10,11] Since almost all of the fluorogenic probes reported thus far are derived from organic dyes, the emission is limited to fluorescence and the utilization is confined to bioimaging. Importantly, photofunctional SNAP-tag substrates that serve as both fluorogenic imaging reagents and photosensitisers for singlet oxygen ($^1O_2$) for cytotoxicity control, to the best of our knowledge, have not been reported.

The rich photophysical properties of iridium(III) polypyridine complexes facilitate their applications as biological probes and imaging reagents for live cells.[12-14] Importantly, their long-lived triplet excited states render these complexes efficient $^1O_2$ photosensitisers for photodynamic therapy.[15,16] We have previously demonstrated that transition metal complexes appended with a nitrone moiety are excellent bioorthogonal phosphorogenic probes for live-cell imaging.[17,18] These complexes are non-emissive due to the efficient non-radiative decay offered by C=N photoisomerisation of the nitrone unit.[19–21] Upon strained promoted alkyne–nitrone cycloaddition (SPANC) with a bicyclononyne (BCN)-modified biomolecule, the nitrone unit is converted into a non-quenching isoxazoline moiety, resulting in intense and long-lived emission and importantly $^1O_2$ photosensitisation (Scheme 1). Thus, both the emission and photocytotoxic activity of the complexes can be readily turned on by SPANC in live cells.

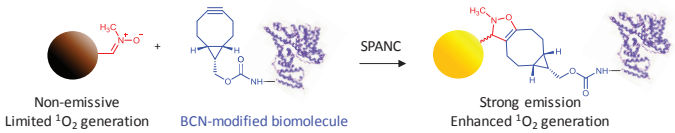

Scheme 1 The SPANC of a transition metal nitrone complex with a BCN-modified biomolecule results in the conversion of the quenching nitrone unit to a non-quenching isoxazoline moiety, turning on the emission and $^1O_2$ photosensitisation of the complex.

Herein we report the modulation of emission and $^1O_2$ photosensitisation in live cells using a new class of iridium(III) polypyridine nitrone complexes [Ir(N^C)$_2$(bpy-nitrone)](PF$_6$) (HN^C = Hbt (**1**), Hbsn (**2**), Hdbq (**3**), Hdbpz (**4**) as bioorthogonal phosphorogenic probes for **BCN-BG** (Scheme 2), which is a specific substrate for SNAP-tag. The synthetic procedures and characterisation data for the complexes and **BCN-BG** are included in the Electronic Supplementary Information. All the complexes were characterised by ESI-MS, ^{1}H NMR and IR spectroscopy, and gave satisfactory elemental analyses.

Upon photoexcitation, the complexes exhibited very weak ($\Phi_{em} < 0.023$) but long-lived ($\tau_o > 0.85$ μs) yellow to red emission in degassed solutions at 298 K (Table S1). Complexes **1** and **2** showed a structured band with a long emission lifetime (τ_o = 2.05 – 3.54 μs), typical of a triplet intraligand (^{3}IL) ($\pi \rightarrow \pi^*$) (N^C) emission origin mixed with some triplet metal-to-ligand

[a] Department of Chemistry, City University of Hong Kong, Tat Chee Avenue, Kowloon, Hong Kong, P. R. China
[b] State Key Laboratory of Terahertz and Millimeter Waves, City University of Hong Kong, Tat Chee Avenue, Kowloon, Hong Kong, P. R. China
[c] Centre of Functional Photonics, City University of Hong Kong, Tat Chee Avenue, Kowloon, Hong Kong, P. R. China
† Electronic Supplementary Information (ESI) available: See
DOI: 10.1039/x0xx00000x

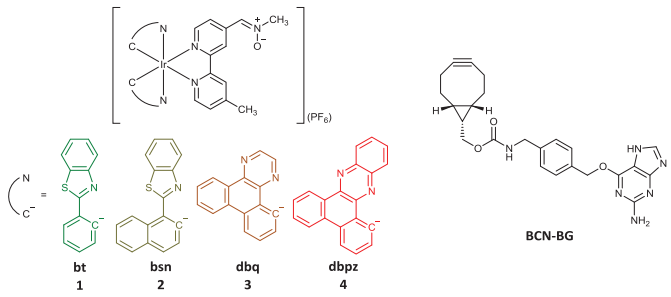

Scheme 2 Structures of complexes **1** – **4** and **BCN-BG**.

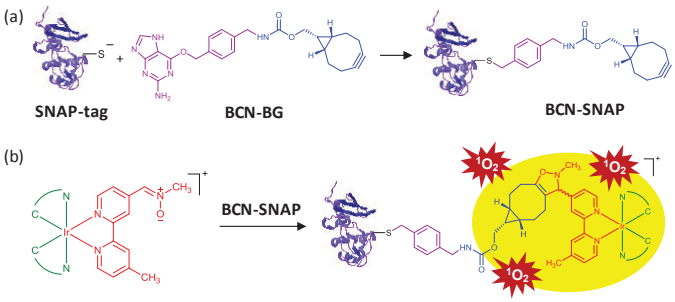

Scheme 3 Modulation of the emission and $^1O_2$ photosensitisation properties of iridium(III) complexes by SPANC: (a) incorporation of **BCN-BG** into SNAP-tag to afford **BCN-SNAP**, (b) SPANC of the nitrone complexes with **BCN-SNAP**.

charge-transfer (^{3}MLCT) (dπ(Ir) $\rightarrow$ π^*(N^C/N^N)) character.[22] In contrast, complexes **3** and **4** displayed a broad band with positive solvatochromism, indicative of a predominantly ^{3}MLCT (dπ(Ir) $\rightarrow$ π^*(N^C/N^N)) parentage of the emission.[23,24] The very low emission quantum yields of the complexes confirmed the efficient quenching of the appended nitrone unit.

The second-order rate constants (k_2) for the complexes with the model strained cyclooctyne, (1*R*,8*S*,9*s*)-bicyclo[6.1.0]non-4-yn-9-ylmethanol (**BCN-OH**), in methanol ranged from 0.189 to 0.270 dm^3 mol^{-1} s^{-1} (Table 1 and Fig. S1), which are larger than that of the free bpy-nitrone ligand (0.040 dm^3 mol^{-1} s^{-1})[17,18] by 4.7 to 6.8 fold. The accelerated rate is a consequence of the positive formal charge of the iridium(III) centre.[17,18] Upon the SPANC, the reaction mixtures showed significant emission enhancement and lifetime extension (I/I_o = 4.5 – 10.1, τ = 0.18 – 0.33 μs, Table 1) as a result of the conversion of the quenching nitrone unit into a non-quenching isoxazoline derivative. Interestingly, the emission enhancement factors were even

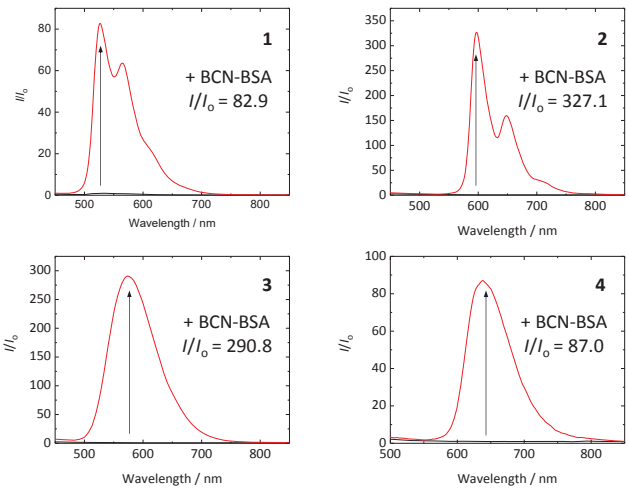

Fig. 1 Emission spectra of complexes **1** – **4** (2.5 μM) in the absence (black) and presence (red) of **BCN-BSA** (2.5 μM) in aerated potassium phosphate buffer (50 mM, pH 7.4)/MeOH (9:1, *v*/*v*) at 298 K. Excitation wavelength = 350 nm.

larger in aqueous buffer (I/I_o = 7.2 – 47.1, τ = 0.28 – 0.58 μs, Table 1 and Fig. S2), attributable to the much weaker emission of the nitrone complexes in aqueous solution before the reaction. As nitrones exhibit spin-trapping behaviour[25] and mild-reactivity towards thiols,[26] the emission intensities of the complexes in the presence of various reactive oxygen/nitrogen species (RONS) and biothiols were examined. We found that all the complexes displayed negligible changes in their emission intensities (Fig. S3), implying that they have excellent selectivity towards strained alkynes.

Bovine serum albumin (BSA) was modified with BCN and the phosphorogenic responses of the complexes towards the resultant conjugate **BCN-BSA** were tested. Impressively, the complexes exhibited significant emission enhancement factors of 82.9 – 327.1 (τ = 0.43 – 1.14 μs) upon reaction with **BCN-BSA** (Fig. 1 and Table 1). This much larger enhancement is ascribed to the hydrophobic local environments of the complexes after the conjugation.[17,18] The formation of the products was confirmed by SDS-PAGE analysis (Fig. S4). Next, we reacted **BCN-BG** with SNAP-tag protein, and isolated and purified the conjugate **BCN-SNAP** (Scheme 3a). As expected, the complexes also displayed more intense emission upon reaction with the conjugate, with the enhancement factors up to 10.6 (τ up to

Table 1 Second-order rate constants, emission enhancement factors (I/I_o),[a] and lifetimes of complexes **1** – **4** upon reactions with **BCN-OH**, **BCN-BSA** and **BCN-SNAP** at 298 K. Unmodified BSA and SNAP-tag were used in the control experiments. The emission lifetimes of complexes **1** – **4** alone in aerated MeOH and aqueous buffer could not be determined with accuracy due to very weak emission.

Complex	**BCN-OH**					**BCN-BSA** (BSA)		**BCN-SNAP** (SNAP-tag)	
	k_2[b]/dm^3 mol^{-1} s^{-1}	I/I_o[b]	τ[b]/μs	I/I_o[c]	τ[c]/μs	I/I_o[c]	τ[c]/μs	I/I_o[c]	τ[c]/μs
1	0.252 ± 0.006	4.5	0.33	7.2	0.58	82.9 (1.5)	0.75 (–)[d]	10.6 (0.4)	0.63 (–)[d]
2	0.270 ± 0.001	10.1	0.29	36.3	0.38	327.1 (2.2)	1.14 (–)[d]	4.5 (1.4)	0.25 (–)[d]
3	0.189 ± 0.002	7.4	0.24	47.1	0.28	290.8 (1.6)	0.57 (–)[d]	1.6 (0.8)	0.22 (–)[d]
4	0.264 ± 0.003	6.3	0.18	16.3	0.35	87.0 (1.2)	0.43 (–)[d]	1.3 (1.1)	–[d] (–)[d]

[a] I_o and I are the emission intensities of the complexes in the absence and presence of **BCN-OH** (250 μM) or proteins (2.5 μM). [Ir] = 10 and 2.5 μM in the **BCN-OH** and protein experiments, respectively. [b] In aerated MeOH. [c] In aerated potassium phosphate buffer (50 mM, pH 7.4)/MeOH (9:1, *v*/*v*). [d] The lifetimes could not be determined with accuracy due to very weak emission.

Table 2 $^1O_2$ generation quantum yields (Φ_Δ) of complexes **1 – 4** and their isoxazoline counterparts in aerated DMSO at 298 K. DPBF was used as the $^1O_2$ scavenger and methylene blue was adopted as the reference.

Complex	Φ_Δ[a]	Φ_Δ[b]
1	0.19	0.42
2	0.25	0.91
3	0.21	0.77
4	0.26	0.67

[a] Φ_Δ of complexes **1 – 4**. [b] Φ_Δ of the isoxazoline counterparts of complexes **1 – 4**.

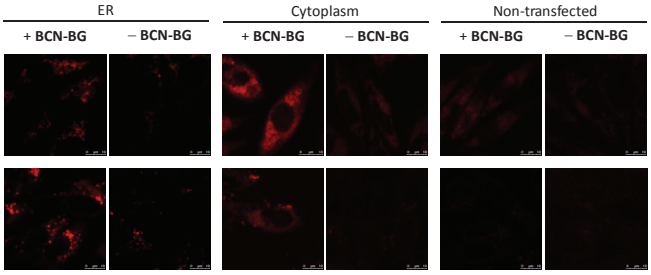

Fig. 2 LSCM images of CHO-K1 cells incubated with complexes **2** and **3** (5 μM) at 37°C for 1 h. Only cells expressing the ER-targeting (left) and cytoplasm-enriched (middle) SNAP-tag with pretreatment of **BCN-BG** (100 μM, 1 h) showed intense emission.

0.63 μs) (Table 1, Scheme 3b). Using complex **1** as an example, the formation of the product was confirmed by SDS-PAGE analysis (Fig. S5). The smaller enhancement compared with **BCN-BSA** could be due to the less hydrophobic environments of the complex after the reaction and possibly a lower MW of the SNAP-tag (19.4 kDa) compared to BSA (66.5 kDa).

The $^1O_2$ generation efficiencies of the nitrone complexes and their isoxazoline counterparts were evaluated in aerated DMSO using 1,3-diphenylisobenzofuran (DPBF) as a $^1O_2$ scavenger.[27] The $^1O_2$ generation quantum yields (Φ_Δ) of transition metal complexes are known to depend on their emission energy,[28] quantum yields[28] and lifetimes.[29] The Φ_Δ values of complexes **1 – 4** were found to be 0.19 – 0.26 while the isoxazoline derivatives displayed higher generation efficiencies of 0.42 – 0.91 (Table 2 and Fig. S6). This indicates that the elimination of nitrone-associated quenching pathway results in much more efficient $^1O_2$ photosensitisation by the complexes due to enhanced emission quantum yields and extended lifetimes.[19–21]

The cellular uptake properties of the complexes were studied using Chinese hamster ovary (CHO)-K1 cells as a model. In particular, the labelling of intracellular SNAP-tag by complexes **2** and **3** was examined. CHO-K1 cells were transfected with phage UbiC SNAP-KDEL[30] and pSNAP$_f$[31] that express endoplasmic reticulum (ER)-targeting and cytoplasm-enriched SNAP-tag, respectively. Laser-scanning confocal microscopy (LSCM) images indicated that strong emission signal was found only in cells that expressed SNAP-tag at ER and cytoplasm (Fig. 2). These observations confirmed that the complexes were facile phosphorogenic probes for labelling intracellular SNAP-tag at different subcellular locations.

The cytotoxicity of the complexes towards the cells in the dark and upon irradiation was examined by the MTT assays and reported as IC_{50} values (Table 3). The effects of (1) the treatment with **BCN-BG** and (2) transfection of the cells to express SNAP-tag in the cytoplasm were evaluated with the use of the phototoxicity index (PI, $IC_{50,dark}/IC_{50,light}$). Towards non-transfected cells, the $IC_{50,dark}$ values for complexes **1** and **2** were about 20 μM, and complexes **3** and **4** were basically non-cytotoxic at [Ir] = 100 and 50 μM, respectively (as limited by their water solubility). Upon photoirradiation, the $IC_{50,light}$ values for all the complexes decreased to 0.64 – 30.9 μM, giving PI of 2.0 – 31.1. The photocytotoxicity is attributable to the $^1O_2$ generation of complexes **1 – 4** in live cells. Upon treatment of the cells with **BCN-BG**, whereas the $IC_{50,dark}$ values were essentially the same, the $IC_{50,light}$ values dropped to a larger extent (0.32 – 21.0 μM), resulting in more pronounced PI of 4.8 – 61.6. These results are in accordance with the more efficient $^1O_2$ generation upon conversion of the nitrone complexes into their isoxazoline counterparts. Remarkably, when the cells had been transfected with the pSNAP$_f$ Vector that expresses SNAP-tag in the cytoplasm, whereas the $IC_{50,dark}$ values were still very similar to those of the non-transfected cells, the $IC_{50,light}$ values substantially decreased to 0.17 – 9.73 μM, leading to a further increase of the PI values to 9.0 – 115.9, indicative of even more enhanced photogeneration of $^1O_2$ when **BCN-BG** and SNAP-tag were co-present.

The cellular uptake efficiency of the complexes was examined with ICP-MS (Table S2). The cellular uptake efficiency of the complexes followed the order: **2** > **1** > **4** > **3**, which is in line with the lipophilicity of the cyclometallating ligands.[17,18,29] More importantly, the cellular uptake of each of the complexes was not significantly changed by pretreatment with **BCN-BG** and transfection of the cells (Table S2). Thus, the larger PI values observed in the transfected cells were due to the higher intracellular concentration of **BCN-BG**, which converts the

Table 3 Cytotoxicity of complexes **1 – 4** towards CHO-K1 cells in the dark and upon irradiation at 365 nm for 30 min. PI is the ratio $IC_{50,dark}/IC_{50,light}$ under different conditions.

Complex	Non-transfected cells without **BCN-BG**			Non-transfected cells with **BCN-BG**[a]			Transfected cells[b] with **BCN-BG**[a]		
	$IC_{50,dark}$/μM	$IC_{50,light}$/μM	PI	$IC_{50,dark}$/μM	$IC_{50,light}$ /μM	PI	$IC_{50,dark}$ /μM	$IC_{50,light}$ /μM	PI
1	20.9 ± 0.7	1.90 ± 0.17	**11.0**	19.5 ± 4.9	1.01 ± 0.01	**19.3**	18.9 ± 0.42	0.34 ± 0.03	**55.6**
2	19.9 ± 4.13	0.64 ± 0.05	**31.1**	19.7 ± 0.89	0.32 ± 0.01	**61.6**	19.7 ± 1.78	0.17 ± 0.02	**115.9**
3	> 100	30.9 ± 0.84	**> 3.2**	> 100	21.0 ± 0.85	**> 4.8**	> 100	9.73 ± 0.75	**> 10.3**
4	> 50	25.0 ± 1.15	**> 2.0**	> 50	7.90 ± 0.51	**> 6.3**	> 50	5.53 ± 0.62	**> 9.0**

[a] Cells were treated with **BCN-BG** (100 μM, 1 h), followed by washing (PBS, 100 μL × 3). [b] Cells had been transfected with the pSNAP$_f$ Vector to express SNAP-tag in the cytoplasm.

nitrone complexes, in a bioorthogonal manner, into their strongly emissive isoxazoline counterparts with enhanced $^1O_2$ photosensitisation and photocytotoxicity.

In conclusion, we developed a strategy to exploit the bioorthogonal reactivity and phosphorogenic property of iridium(III) polypyridine nitrone complexes and SNAP-tag for the modulation of emission and $^1O_2$ photosensitisation in live cells. Utilisation of the strained alkyne-containing substrate **BCN-BG** allows the complexes to serve as phosphorogenic probes to target SNAP-tag at different subcellular locations. Additionally, **BCN-BG** and SNAP-tag significantly increase the $^1O_2$ photosensitisation and hence photocytotoxicity of the complexes. Although related work on fluorogenic imaging reagents and photosensitisers for $^1O_2$ based on organic compounds has been reported,[32,33] this study involves the use of phosphorogenic transition metal complexes as bioorthogonal probes for photocytotoxicity modulation. One obvious advantage is the facile population of a long-lived triplet excited state, which is an excellent $^1O_2$ photosensitiser. Another uniqueness is the use of SNAP-tag to provide localisation selectivity, which allows emission and photocytotoxicity turn-on at specific subcellular locations. The two-step labelling process in this study is expected to allow greater adaptability, since other protein tags and bioorthogonal handles can be used simultaneously to allow multiplexed applications. We believe that the combined strategy of bioorthogonal reactivity, photofunctional switching, and protein tag technology will lead to the development of new theranostic applications.

This work was funded by the Hong Kong Research Grants Council (Project No. CityU 11300019, CityU 11300318, CityU 11300017, CityU 11302116 and T42-103/16-N). P.K.-K.L. acknowledges the receipt of a Postgraduate Studentship and Outstanding Teaching Awards for Teaching Assistants, both administered by City University of Hong Kong.

Conflicts of interest

There are no conflicts to declare.

References

1 See, for example: (a) M. J. Hinner and K. Johnsson, *Curr. Opin. Biotechnol.*, 2010, **21**, 766–776; (b) C. Jing and V. W. Cornish, *Acc. Chem. Res.*, 2011, **44**, 784–792.
2 A. Keppler, S. Gendreizig, T. Gronemeyer, H. Pick, H. Vogel and K. Johnsson, *Nat. Biotechnol.*, 2003, **21**, 86–89.
3 S. A. Jones, S.-H. Shim, J. He and X. Zhuang, *Nat. Methods*, 2011, **8**, 499–505.
4 D. Maurel, L. Comps-Agrar, C. Brock, M.-L. Rives, E. Bourrier, M. A. Ayoub, H. Bazin, N. Tinel, T. Durroux, L. Prézeau, E. Trinquet and J.-P. Pin, *Nat. Methods*, 2008, **5**, 561–567.
5 A. Gautier, E. Nakata, G. Lukinavičius, K. T. Tan and K. Johnsson, *J. Am. Chem. Soc.*, 2009, **131**, 17954–17962.
6 E. Tomat, E. M. Nolan, J. Jaworski and S. J. Lippard, *J. Am. Chem. Soc.*, 2008, **130**, 15776–15777.
7 A. Keppler and J. Ellenberg, *ACS Chem. Biol.*, 2009, **4**, 127–138.
8 I. R. Corrêa, Jr., *Curr. Opin. Chem. Biol.*, 2014, **20**, 36–45.
9 S. Leng, Q.-L. Qiao, Y. Gao, L. Miao, W.-G. Deng and Z.-C. Xu, *Chinese Chem. Lett.*, 2017, **28**, 1911–1915.
10 A. Nadler and C. Schultz, *Angew. Chem. Int. Ed.*, 2013, **52**, 2408–2410.
11 Y. Hori and K. Kikuchi, *Curr. Opin. Chem. Biol.*, 2013, **17**, 644–650.
12 K. K.-W. Lo, *Acc. Chem. Res.*, 2020, **53**, 32–44.
13 C. Caporale and M. Massi, *Coord. Chem. Rev.*, 2018, **363**, 71–91.
14 K. Qiu, Y. Chen, T. W. Rees, L. Ji and H. Chao, *Coord. Chem. Rev.*, 2019, **378**, 66–86.
15 D. Ashen-Garry and M. Selke, *Photochem. Photobiol.*, 2014, **90**, 257–274.
16 L. K. McKenzie, H. E. Bryant and J. A. Weinstein, *Coord. Chem. Rev.*, 2019, **379**, 2–29.
17 L. C.-C. Lee, J. C.-W. Lau, H.-W. Liu and K. K.-W. Lo, *Angew. Chem. Int. Ed.*, 2016, **55**, 1046–1049.
18 T. S.-M. Tang, H.-W. Liu and K. K.-W. Lo, *Chem. Eur. J.*, 2016, **22**, 9649–9659.
19 J.-S. Wu, W.-M. Liu, X.-Q. Zhuang, F. Wang, P.-F. Wang, S.-L. Tao, X.-H. Zhang, S.-K. Wu and S.-T. Lee, *Org. Lett.*, 2007, **9**, 33–36.
20 X. Cheng, H. Jia, T. Long, J. Feng, J. Qin and Z. Li, *Chem. Commun.*, 2011, **47**, 11978–11980.
21 M. Üçüncü and M. Emrullahoğlu, *Chem. Commun.*, 2014, **50**, 5884–5886.
22 K. K.-W. Lo, C.-K. Li and J. S.-Y. Lau, *Organometallics*, 2005, **24**, 4594–4601.
23 X. Li, H. Lan, Y. Chen, K. Lv, A. Zhang and T. Huang, *Inorg. Chim. Acta*, 2012, **390**, 41–46.
24 T. Bura, P. Retailleau, M. T. Indelli and R. Ziessel, *Dalton Trans.*, 2013, **42**, 4544–4551.
25 C. L. Hawkins and M. J. Davies, *Biochim. Biophys. Acta*, 2014, **1840**, 708–721.
26 E. G. Bagryanskaya, O. A. Krumkacheva, M. V. Fedin and S. R. A. Marque, *Methods Enzymol.*, 2015, **563**, 365–396.
27 N. Adarsh, R. R. Avirah and D. Ramaiah, *Org. Lett.*, 2010, **12**, 5720–5723.
28 J. S. Nam, M.-G. Kang, J. Kang, S.-Y. Park, S. J. C. Lee, H.-T. Kim, J. K. Seo, O.-H. Kwon, M. H. Lim, H.-W. Rhee and T.-H. Kwon, *J. Am. Chem. Soc.*, 2016, **138**, 10968–10977.
29 S. P.-Y. Li, C. T.-S. Lau, M.-W. Louie, Y.-W. Lam, S. H. Cheng and K. K.-W. Lo, *Biomaterials*, 2013, **34**, 7519–7532.
30 F. Voigt, H. Zhang, X. A. Cui, D. Triebold, A. X. Liu, J. Eglinger, E. S. Lee, J. A. Chao and A. F. Palazzo, *Cell Rep.*, 2017, **21**, 3740–3753.
31 The plasmid pSNAP$_f$ Vector was obtained from New England Biolabs. See, https://international.neb.com/products/n9183-psnapf-vector, (accessed March 2020).
32 W. Lv, S. Chi, W. Feng, T. Liang, D. Song and Z. Liu, *Chem. Commun.*, 2019, **55**, 7037–7040.
33 Y. Zhou, R. C. H. Wong, G. Dai and D. K. P. Ng, *Chem. Commun.*, 2020, **56**, 1078–1081.

